materials

MDPI

Article

Enhanced Microstructural and Mechanical Properties of Mig Welded Al 7075 Alloy Under Longitudinal Vibrations

Teodor Machedon-Pisu [1] and Mihai Machedon-Pisu [2,*]

[1] Department of Materials Engineering and Welding, Transilvania University of Brașov, B-dul Eroilor nr. 29, 500036 Brașov, Romania; tmache@unitbv.ro
[2] Department of Electronics and Computers, Transilvania University of Brașov, B-dul Eroilor nr. 29, 500036 Brașov, Romania
* Correspondence: mihai_machedon@unitbv.ro

Abstract

In many areas such as the automotive, aircraft, and building industries, the high-strength aluminum alloy Al 7075 is frequently used due to its appropriate properties as a lightweight structural material. However, due to modest weldability, it is challenging to obtain high-quality welds with suitable mechanical properties, as cracks are generated while welding. Moreover, in order to avoid post-welding heat treatments and the use of complex welding equipment, in this paper the Al 7075 alloy is welded with MIG under longitudinal vibrations by using the Al 4043 alloy as filler material. As a consequence of strengthening the HAZ through precipitation, the mechanical and structural properties of the welded joints can be improved. These are investigated both under longitudinal forced vibrations at 50 Hz and without such vibrations. The results reveal improvements in terms of reducing the risk of hot cracking, obtaining a band structure free of porosity of the welds, improving the hardness of the welds under vibrations by 8.7% to 12.5%, and improving the tensile strength of the plates welded under vibrations by 12 to 15.5% in comparison to no vibrations. In relation to other welding procedures, the proposed procedure is more cost-effective and the weld quality is improved during the welding process.

Keywords: mechanical properties; microstructural characteristics; Al 7075 alloy; metal inert gas (MIG) welding; longitudinal vibrations; heat-affected zone (HAZ)

Academic Editor: Chih-Chun Hsieh

Received: 21 August 2025
Revised: 2 September 2025
Accepted: 10 September 2025
Published: 12 September 2025

Citation: Machedon-Pisu, T.; Machedon-Pisu, M. Enhanced Microstructural and Mechanical Properties of Mig Welded Al 7075 Alloy Under Longitudinal Vibrations. *Materials* **2025**, *18*, 4281. https://doi.org/10.3390/ma18184281

1. Introduction

The use of aluminum is closely related to the cumulative benefits that it offers in many industrial areas such as aerospace, the automotive industry, construction, machinery, sensors, and the military [1–10]. These benefits include reduced cost, low density, high thermal conductivity and anticorrosion [3,6–8,11]. High-strength aluminum alloys belonging to the 7xxx series are widely used as lightweight structural materials presenting excellent properties related to specific strength, toughness, stiffness, hardness, machining performance, and corrosion resistance [2–4,6–10,12].

The aluminum 7xxx series is a heat-treatable group of alloys that incorporate both weldable and non-weldable chemical compositions [2,5,12–14]. In order to meet the corresponding internal standards and norms, it must be mentioned that high-quality welds of these aluminum alloys are a key element in manufacturing automotive and aircraft structure components, as noticed in a few studies [4,5]. Improvements in this field without heat treatments or complex welding equipment [11,15,16] are important due to the need

to scale down production costs, as noticed in [10]. This also leads to a higher efficiency in time spent, as well as offering capabilities such as pollution control and energy savings, as depicted in [12,14]. Other relevant aspects related to the above-mentioned issues refer to improvements in fatigue response [11,15,17–19], machinability [20], strengthening [17,21–28], corrosion resistance [23,28], productivity [29], wear resistance [29], and stability [30].

However, the advantages that certain aluminum alloys from the 7xxx series bring as a consequence of their physical, chemical and mechanical properties can be compromised when trying to use them in technical environments for which they have not been designed. This is especially the case with the AlZn5.5MgCu alloy, otherwise known as the 7075 series or the Al 7075 alloy, which is a heat-treatable alloy with impressive tensile and yield strength [4,6,8,12] but with poor weldability [5,12,13]. The most widely used technologies for welding Al 7075 alloys are tungsten inert gas (TIG) [13,23,25] and metal inert gas (MIG) welding [5,11], plasma arc welding [21], laser welding [6,12,17], and friction stir welding (FSW) [14–16,18,24,26]. Although FSW has gained a lot of interest recently, most studies do not consider the negative impact on production and labor costs, the requirements which result from the use of expensive welding devices [14,18,26], or post-welding treatments [15,16,24]. Such expenses, among others such as consumables and maintenance costs, are also relevant in the case of plasma arc welding and laser welding [6]. Both TIG and MIG are better suited when it comes to lower costs and higher productivity [23,25], with MIG being slightly better in productivity [5].

A large number of research studies focus on the analysis of structural and mechanical characteristics of Al 7075 welded joints in terms of microstructure [17,21,24,25,27,31–41], hardness [17,21,26,33,34,36,42–45], grain structure [22,26,40,44–47], and mechanical properties [16,17,21,25,32,34–36,38–40,42,47–50], as well as cracks [5,18,37,51,52], residual stress [53], and elastic-plastic strain [54]. Also, non-conventional measurement methods can be applied in this regard, such as in [55].

It can be noticed that in many of these studies, such as [6,11,12,14–18,21–25,27,31,36,38,39,42,44,47,50,54], post-processing treatments are applied in order to improve the structural and mechanical characteristics of Al 7075 welded joints. Out of the mentioned studies, only [36] does not treat any aspect regarding the generation of cracks.

At the same time, it must be mentioned in this regard that the majority of these studies fail to emphasize the technical aspects regarding mechanical vibrations that can have a significant influence on microstructure and, implicitly, on the evolution of cracks. Yet a few studies mention these aspects, such as [23,29,30,39,45,54]. Vibrations are shown to have an influence on the grain structure in [23,54]. The effects of ultrasonic vibrations on mechanical properties are mentioned in [39,45].

In terms of microstructure analysis, which is related to the presence of cracks in aluminum 7xxx series welded joints, it is well-known that alloys like Al, Zn, and Mg have a higher tolerance to hot cracking and show better welding performances, in comparison to Al, Zn, Mg, and Cu alloys [56,57]. In Al, Zn, and Mg alloys, the quantity of magnesium increases the sensitivity to cracking, a reaction that can be reduced by adding zirconium, in order to obtain a more refined grain size structure, thus improving the mechanical properties of the weld, as shown in [2,58].

In relation to MIG welding feasibility, the Al 7075 alloy can be affected by stress corrosion cracking, which is why it is not usually welded, as the propensity to crack while welding occurs due to the compound of Cu with Zn and Mg in the alloy, thus intensifying the solidification stress and leading to grain boundaries cracking, as discussed in [59]. As a difference, an alloy such as Al 7003, which has a small amount of copper (between 0.2% and 0.4%), is specially designed for high-strength welding [60]. Although the Al 7075 alloy is considered unsuitable for welding because of its increased probability of stress-induced

corrosion [8], its physical characteristics are very interesting despite its low density of 2.81 g/cm^3 [11].

It is worth mentioning that one important property of all 7xxx alloys is the capacity of the heat-affected zone (HAZ) to become strengthened through precipitation after welding through post-welding treatments, as discussed in numerous studies [4,9–15,18,19,21,24,25,27,32,34,36–38,41,42,44,46–50,58,59]. In many of these studies, the authors manage to obtain a decrease in the size of grains by reducing the HAZ.

As mentioned previously in [23,29,30,39,45,54], the presence of mechanical vibrations at various frequencies can also affect the grain structure. By manipulating the frequency, there is an obvious difference in structure with new sets of different characteristics. The differentiation of property efficiency can be established as efficiently as possible by starting from the classic welding procedure and moving toward a level of influence in the vibration frequency of the weld, which can highlight the reactions that occur. In this regard, a reduction in hot cracking in the susceptible area of an Al 7075 weld with TIG and MIG was observed by authors in [61] by subjecting it to mechanical vibrations at frequencies of 1025 and 2050 Hz, which has also led to a superior refinement of the structure in comparison to welding at higher and lower frequencies. Ultrasonic vibrations (beyond 20 kHz) have been applied during TIG welding of Al 5A06, Al 5A02 and Al 4047 in [62], revealing an increase in joint strength as well as increased microhardness in both the HAZ and the weld, as a consequence of grain refinement. Another study [63] discusses ultrasonic vibrations during welding of aluminum alloys from 5xxx and 6xxx series in terms of bonding for achieving proper welding, also addressing the major limitation of ultrasonic welding regarding its power delivery capability.

By carrying out MIG welding with longitudinal vibrations at lower frequencies, such as 52 Hz in [64] for an Al 6082 alloy, it was shown that weld solidification can have a major influence on the quality of the joining material, leading to finer and more uniform grains and better hardness in both the HAZ and the weld. Another study that applied vibrations during MIG welding [65] but at a lower frequency (10 Hz for an Al 6061 alloy) has shown that the grain growth of HAZ is slowed down and the influence of heat input on the base metal is decreased, also increasing the hardness in the base metal and the HAZ.

As shown in [66], coarse-grained structures (dendrites) appear in welds without forced vibrations. It can be interpreted that vibrations can improve the structural and mechanical properties of welded joints, as presented previously in [23,39,54,61–66]. But, in order to create beneficial changes in the metallographic structure of the welded joints with the contribution of longitudinal vibration, it is imperative to have permanent control over the vibrational course and its direction, and also to control the thermal influences. Various studies focused on this area describe various ways of introducing forced vibrations into the weld bed, such as electric arc vibrations [67,68] or introducing waveguide forced vibrations [69]. Mechanical vibrations can lead to beneficial structural changes and improve mechanical features of the finished material. The authors highlight the fact that full control is present during welding, without requiring any post-welding treatments.

In this study the authors apply forced longitudinal mechanical vibrations to an Al 7075 alloy welded with MIG at frequencies around 50 Hz. As a consequence, the mechanical and structural properties of the welded joints are investigated within.

2. Materials and Methods

The study has the comparative purpose to identify the mechanical, physical and chemical properties of the welds obtained with and without vibrations. In this regard, the experimental procedure consists of the mechanized welding on a ceramic support of two sets of Al 7075 (AlZn5.5MgCu, Alro S.A., Slatina, Romania) plates with dimensions of

300 mm × 150 mm × 10 mm. MIG welding equipment [70] is placed on a vibrating surface with a mechanized linear welding torch manipulator used in straight line welding. The MIG equipment (Air Liquide, Paris, France) was set to a 4-tact welding setup so that the beginning of the electric arc and the start of the welding torch travel were synchronized accordingly. For both procedures of welding, with and without vibrations, the welding torch was fixed on the arm of the mechanized equipment and positioned vertically so it could perform flat welding.

The Al 7075 experimental specimens that were to be welded were clamped on a metallic platform that had springs at every corner. To the vibrating metallic plate, an electrodynamic exciter was attached, in order to propagate vibrations in to the platform. The vibrating platform oscillates horizontally in the same direction as the weld is formed with a frequency-dependent acceleration. To power and control the electrodynamic vibration system, the authors used a power amplifier, a low-frequency generator with a frequency control system, a multimeter and frequency measurement system, in order to ensure the right frequency. The induced longitudinal vibration parameter used in the analysis has a frequency of 50 Hz. In accordance with recommendations of specialized companies and validations from industrial experience, the values for the experimental and technical welding parameters are determined as presented in Table 1, where I is the welding current, U is the supply voltage, f is the welding frequency, S is the welding speed, Sfw is the filler material speed, and Q Argon is the Argon gas flow.

Table 1. Technical welding characteristics.

Specimen	I [A]	U [V]	f [Hz]	S [cm/min]	Sfw [m/min]	Q Argon [L/min]
Al 7075, vibrated	192	20	50	45	8.1	15
Al 7075, stationary	192	20	–	45	8.1	15

The chemical composition of the Al 7075 alloy is given in Table 2.

Table 2. Chemical composition of the Al 7075 alloy (AlZn5.5MgCu) welded in the experiment.

Alloy Designation	Si	Fe	Cu	Mn	Mg	Cr	Zn	Ti	Others (%)
EN AW-7075 *	Max. 0.4	Max. 0.5	1.2–2	Max. 0.3	2.1–2.9	0.18–0.28	5.1–6.1	Max. 0.2	Max. 0.15

* According to SR EN 573-3 [71].

For the welding procedure the authors used the Al 4043 alloy (AlSi5, Air Liquide, Paris, France) as filler material. Its chemical composition is depicted in Table 3.

Table 3. Chemical composition of the Al 4043 alloy (AlSi5) used as filler material.

Alloy Designation	Si	Fe	Cu	Mn	Mg	Zn	Ti	Ga	Others (%)
EN AW-4043A *	4.5–6	Max. 0.8	Max. 0.3	Max. 0.05	Max. 0.05	Max. 0.1	Max. 0.2	-	0.05

* According to SR EN 573-3 [71].

Al 4043, or AlSi5, is a 4xxx series aluminum silicon-based alloy that contains a high level of silicon, as depicted in Table 3. By alloying aluminum with silicon, the

alloy is given a set of properties with specific characteristics, such as reduced melting point [12,59] and excellent weldability [12]. Moreover, it improves the fluidity of the molten metal [12,32]. This is the reason why this alloy is especially used as filler material, as presented in [32,59,64,72–74]. Silicon, independently of aluminum, does not respond well to high temperatures, as noticed in [32], but some of these silicon alloys have been produced with additions of magnesium and copper, which enhance the ability to respond favorably to high-temperature welding, as shown in [12,32]. Silicon-based filler metals such as Al 4043 alloy (AlSi5) are not suitable for welding alloys like Al 7075 (AlZn5.5MgCu), since the Si surplus introduced by the filler wire leads to the formation of excessive quantities of fragile Mg_2Si grains in the weld, as noticed in [12,32,59]. Most of the studies mentioned previously, such as [4,9–15,18,19,21,24,25,27,32,34,36–38,41,42,44,46–50,58,59], apply heat treatments after welding in order to strengthen the alloy by the precipitation of Mg_2Si, as highlighted in [32]. However, in this study the strengthening occurs during welding. In this regard, the strength of a weld is established based on its size and by the shear strength of the filler metal used. In aluminum welding it is possible to select one of several different filler alloys to weld a particular aluminum alloy, with the most suited candidates as filler material being Al 4047 [75], 4643 [76], 5183 [77,78], 5356 [32,73], and 5554 [79], besides Al 4043. Based on the characteristics of the weld standpoint, it should be mentioned that in selecting the correct filler metal, the shear strength is an important factor, as depicted in [80,81]. From the comparison in Table 4, it can be noticed that the Al 4043 alloy has a lower level of shear strength, especially when compared to 5xxx series [82].

Table 4. Longitudinal shear strength comparison of aluminum filler alloys.

Filler Alloy	Longitudinal Shear Strength (MPa)
4043	80
4047	80–90
4643	93
5183	127.6
5356	117.2
5554	103.4

The superior mechanical resistance characteristic of the Al 7075 alloy and the capability of the HAZ to become strengthened through precipitation, in combination with the high fluidity of the Al filler material 4043, create a suitable environment for the alloy elements in the Al 7075 base material to precipitate in the HAZ of a weld formed with a lower-melting-point alloy that can withstand high temperatures due to additions of Mg and Cu. By introducing forced longitudinal vibrations in to the weld bed, the authors predict that the risk of hot cracking can be reduced, as discussed in [59], and a lower level of hydrogen inclusions in a higher-density grain microstructure (fragile Mg_2Si grains) can be obtained, which is desired in [12,32,59].

In this regard, from each welded plate on a flat ceramic surface, the following samples were taken for laboratory mechanical tests and macroscopic and microscopic examinations:

- Two specimens of each welding procedure for macroscopic and microscopic examination;
- Two specimens of each welding process for the Vickers HV 100 microhardness test;
- Three specimens of each welding procedure, cut with water jets, according to ISO 4136: 2013 [83] dimensions for a transverse tensile test;
- Two specimens of each welding procedure for SEM coupled with EDX analysis (TESCAN, Brno, Czech Republic).

3. Results

Figure 1 represents photographs of MIG fusion weld structures of the test samples without and with forced longitudinal vibrations.

(**a**) (**b**)

Figure 1. Macroscopic image of the test specimens welded: (**a**) without vibrations; (**b**) with vibrations; magnification: 10×.

It can be observed in Figure 1a that the MIG welding procedure without vibrations consists in a considerable growth in the number of gaseous pores.

3.1. Chemical Composition Concentrations and Elemental Mapping Analysis

The chemical composition concentrations of the cross-section of the weld and base material produced by MIG welding in terms of metallic elements in the two cases, without and with vibrations, are presented in Figures 2 and 3, together with a Scanning Electron Microscopy (SEM) image.

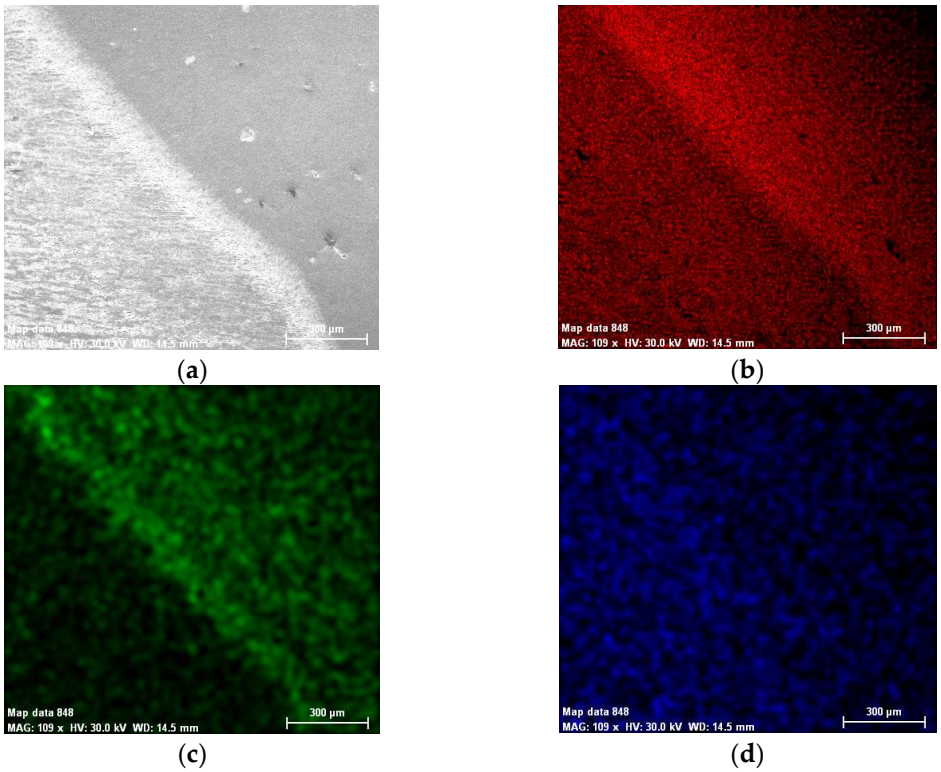

(**a**) (**b**)

(**c**) (**d**)

Figure 2. *Cont.*

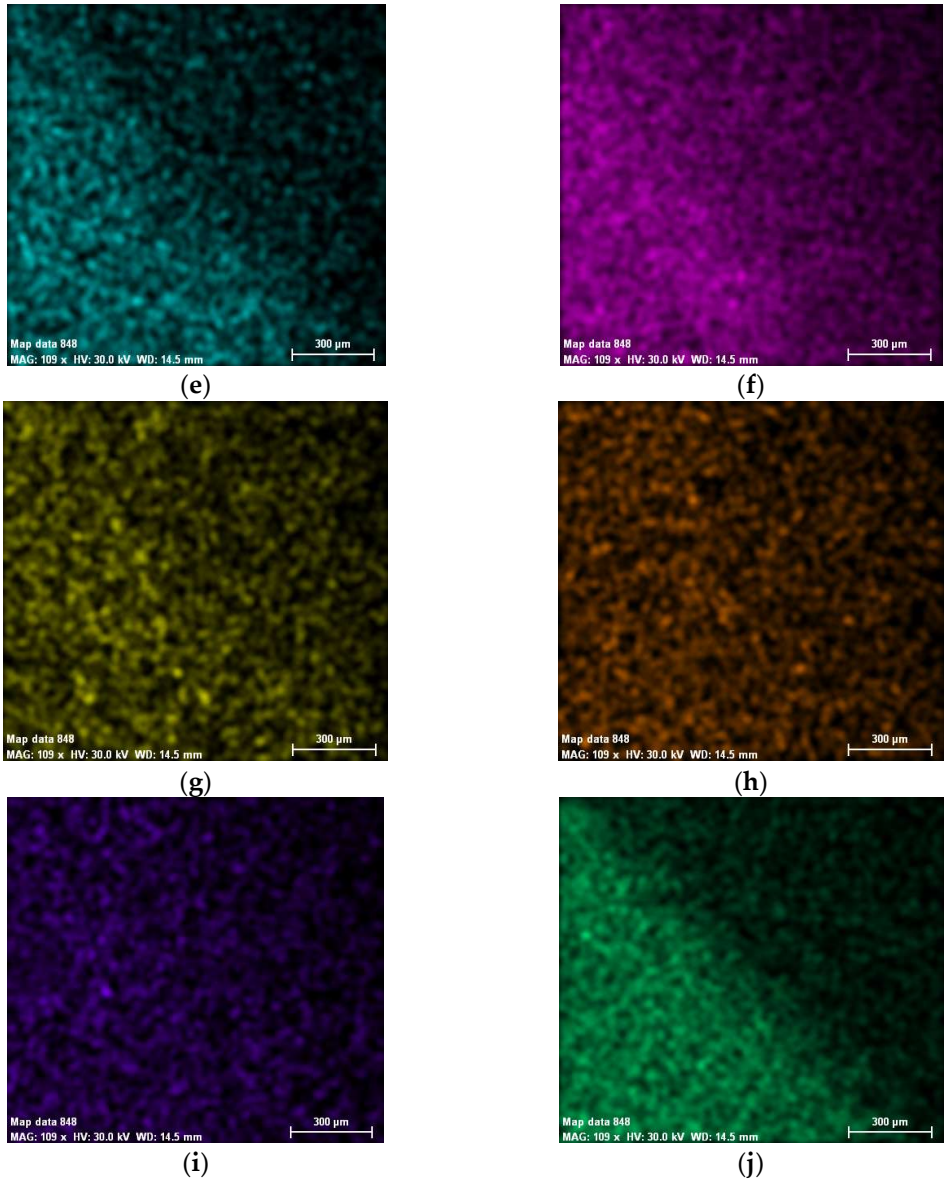

Figure 2. Chemical composition concentrations of the cross-section of the weld produced by MIG welding without longitudinal vibrations: (**a**) SEM image; (**b**) Al; (**c**) Si; (**d**) Cr; (**e**) Cu; (**f**) Mg; (**g**) Fe; (**h**) Ti; (**i**) Zn; (**j**) Mn.

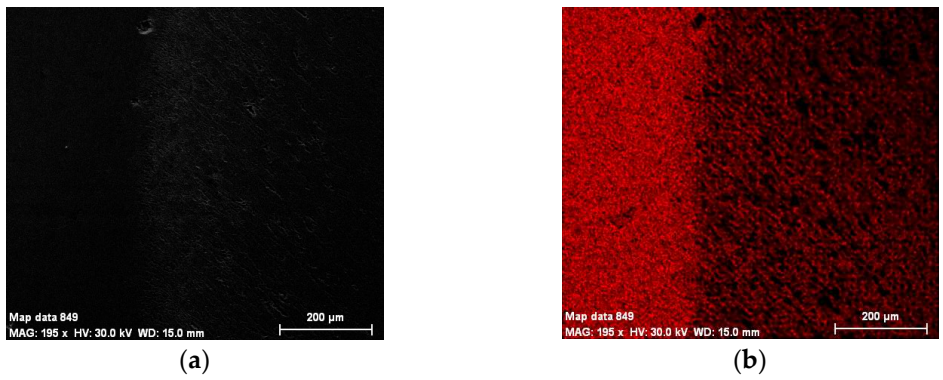

Figure 3. *Cont.*

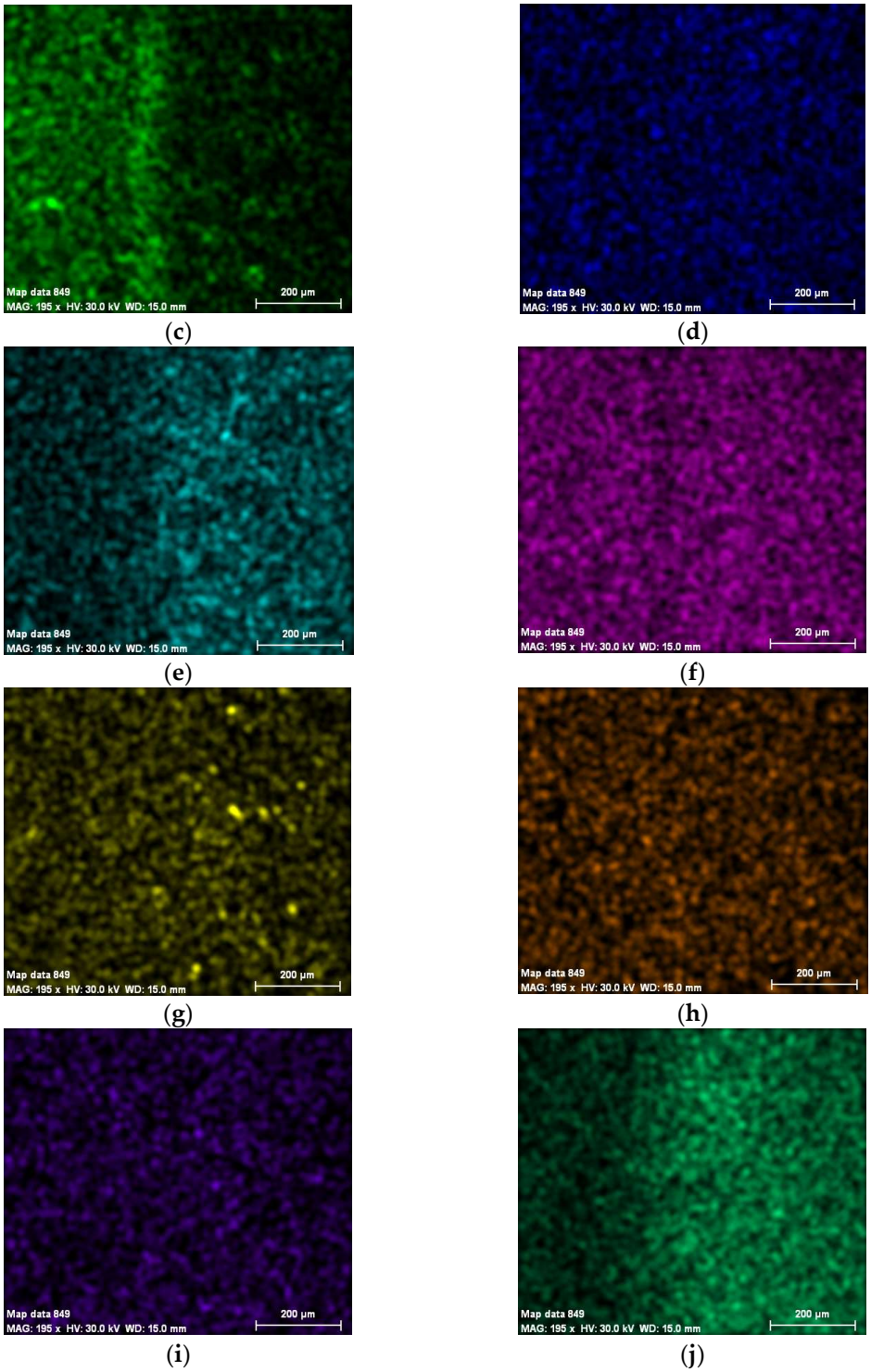

Figure 3. Chemical composition concentrations of the cross-section of the weld produced by MIG welding with longitudinal vibrations: (**a**) SEM image; (**b**) Al; (**c**) Si; (**d**) Cr; (**e**) Cu; (**f**) Mg; (**g**) Fe; (**h**) Ti; (**i**) Zn; (**j**) Mn.

In MIG welding, the subsequent stages of solidification of the molten pool are visible in Figure 4, being represented by the lighter-color lines arranged circumferentially at every few µm beginning from the fusion line up to the weld face boundary.

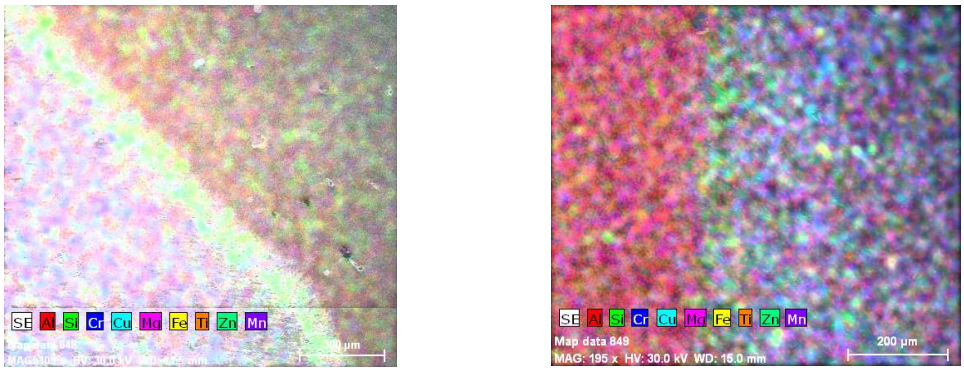

(**a**) (**b**)

Figure 4. Composite elemental map in the weld produced by MIG welding: (**a**) without vibrations; (**b**) with vibrations.

The metallic compositions obtained in the weld in the two cases, without and with longitudinal vibrations, are depicted according to Figures 5 and 6.

(**a**)

(**b**)

Figure 5. Chemical composition concentrations (in number of counts) in the weld produced by MIG welding without longitudinal vibrations of (**a**) metallic elements and (**b**) metallic elements except Al.

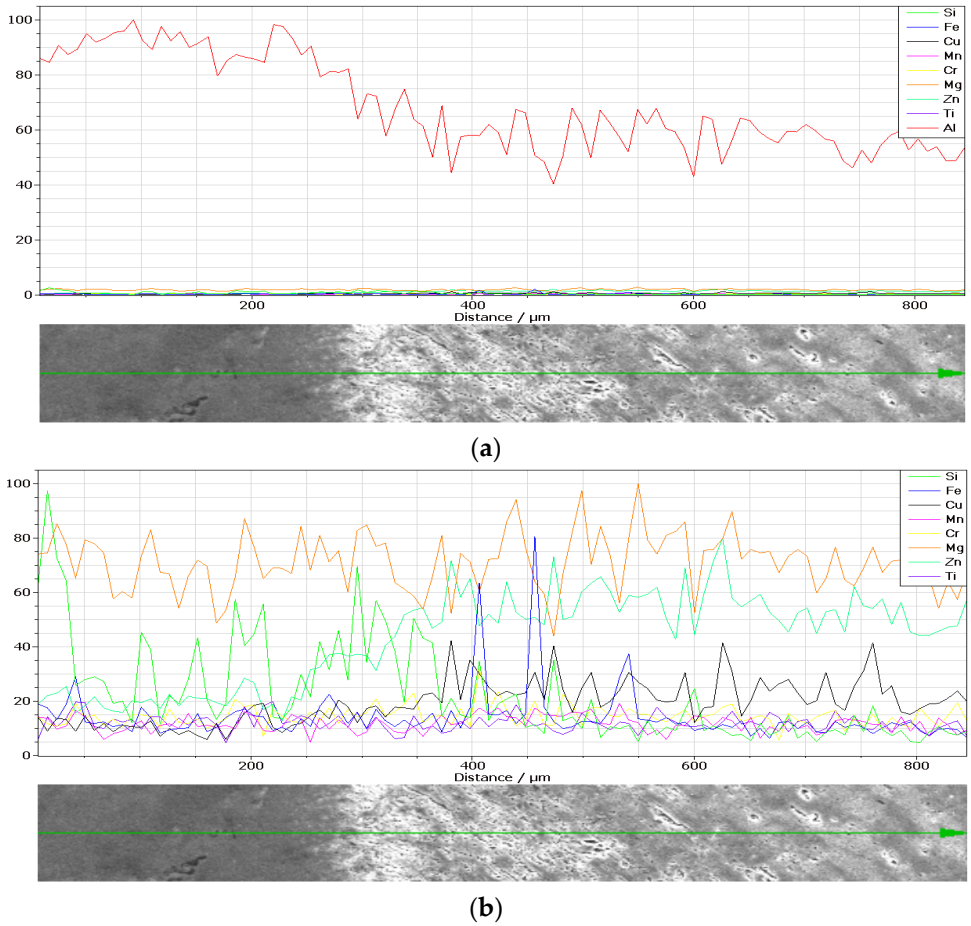

Figure 6. Chemical composition concentrations (in number of counts) in the weld produced by MIG welding with longitudinal vibrations of (**a**) metallic elements and (**b**) metallic elements except Al.

By normalizing the metallic chemical concentrations depicted in Figures 5 and 6 in number of counts, the experimental concentrations are determined in Tables 5 and 6 in percent.

Table 5. Chemical composition (%) of the Al 7075 alloy (AlZn5.5MgCu) determined experimentally without vibrations.

Alloy Designation	Si	Fe	Cu	Mn	Mg	Cr	Zn	Ti
EN AW-7075 *	1.6	0.5	0.92	0.2	2	0.15	3.5	0.18

* MIG welded without vibrations.

Table 6. Chemical composition (%) of the Al 7075 alloy (AlZn5.5MgCu) determined experimentally with vibrations.

Alloy Designation	Si	Fe	Cu	Mn	Mg	Cr	Zn	Ti
EN AW-7075 *	2	0.6	1	0.22	2.5	0.18	3	0.16

* MIG welded with vibrations.

3.2. Scanning Electron Microscopy of the HAZ and Cross-Section of the Welds

The cross-sections of the HAZ and weld's morphology are examined in detail by using SEM in Figures 7–9.

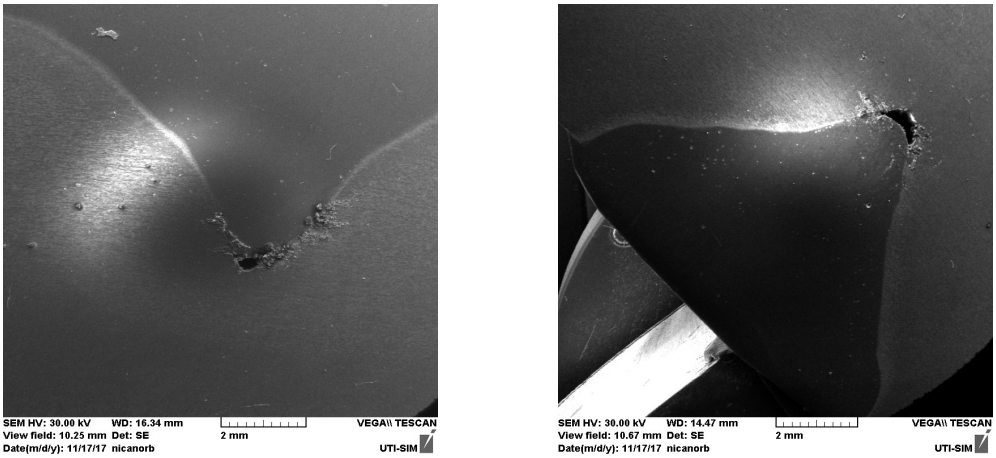

(**a**) (**b**)

Figure 7. Microstructure in the HAZ of the MIG weld: (**a**) without longitudinal vibrations; (**b**) with longitudinal vibrations; magnification 20×.

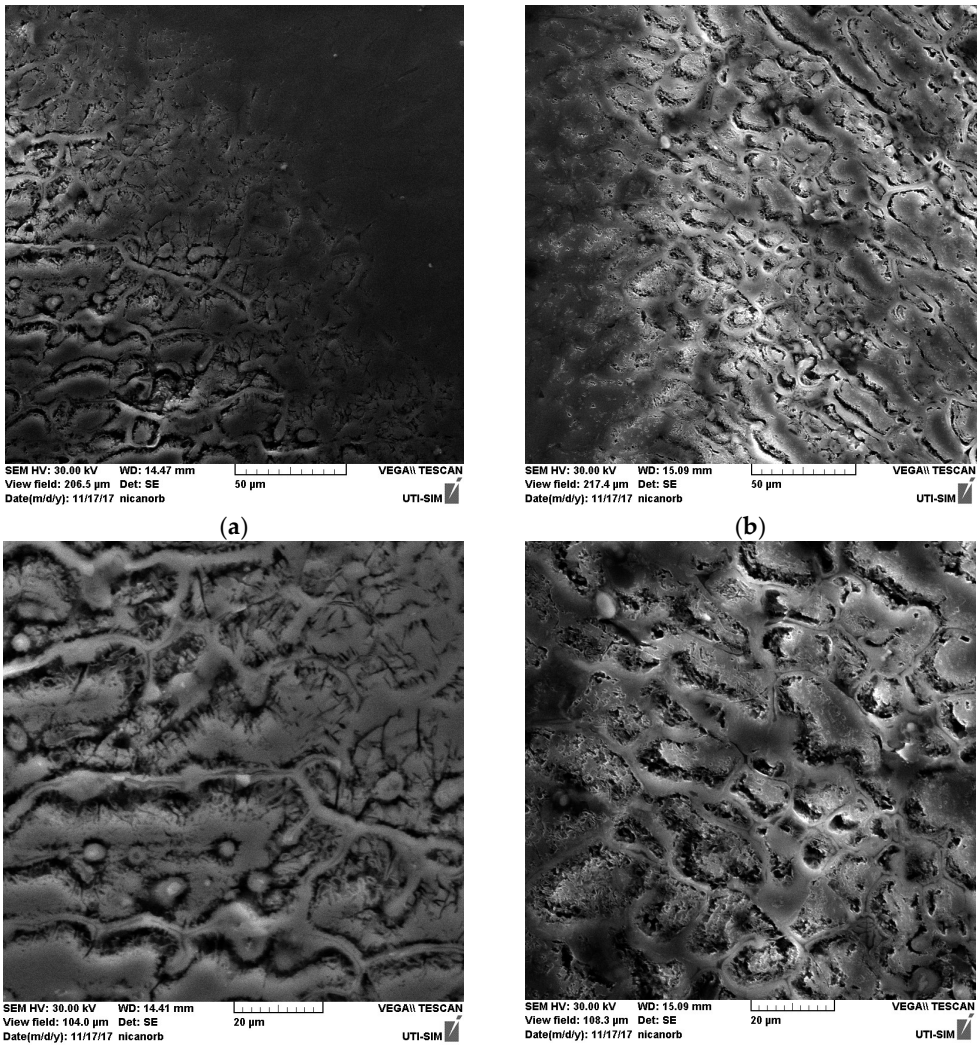

(**a**) (**b**)

(**c**) (**d**)

Figure 8. *Cont.*

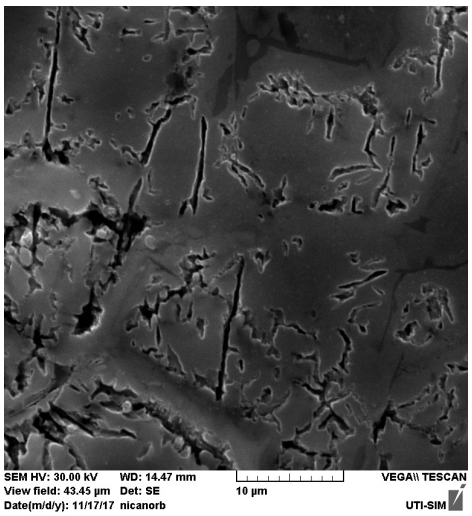

(**e**) (**f**)

Figure 8. Microstructure in the HAZ of the MIG weld, magnification: (**a**) 1000×, without vibrations; (**b**) 1000×, with vibrations; (**c**) 2000×, without vibrations; (**d**) 2000×, with vibrations; (**e**) 5000×, without vibrations; (**f**) 5000×, with vibrations.

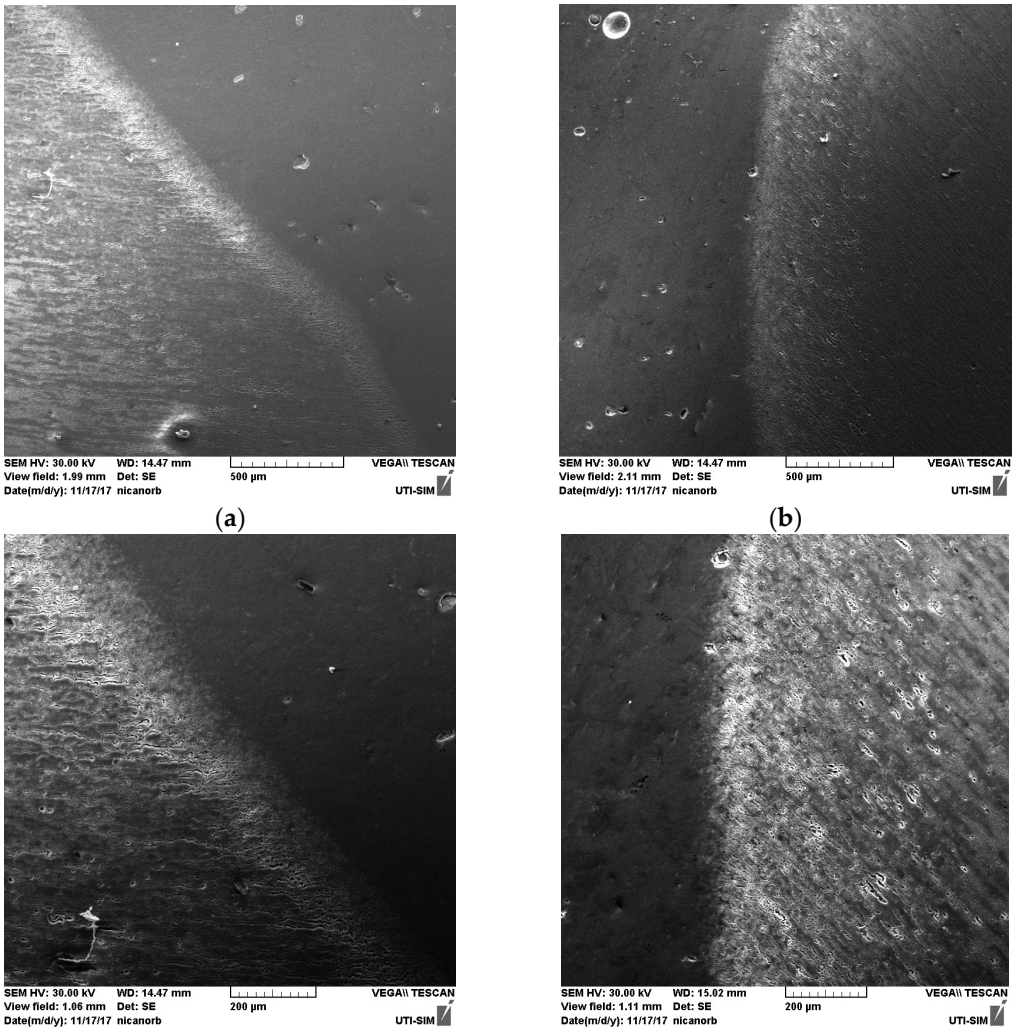

(**a**) (**b**)

(**c**) (**d**)

Figure 9. *Cont.*

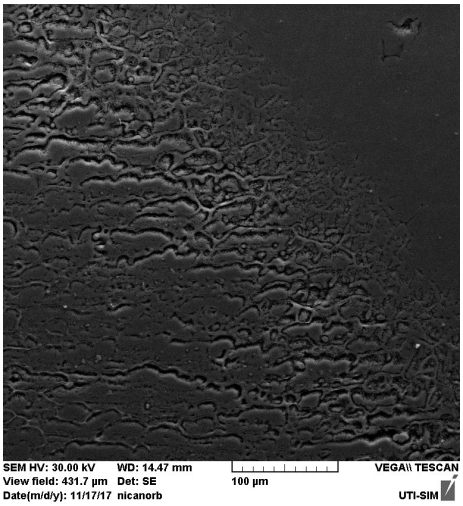

(**e**)

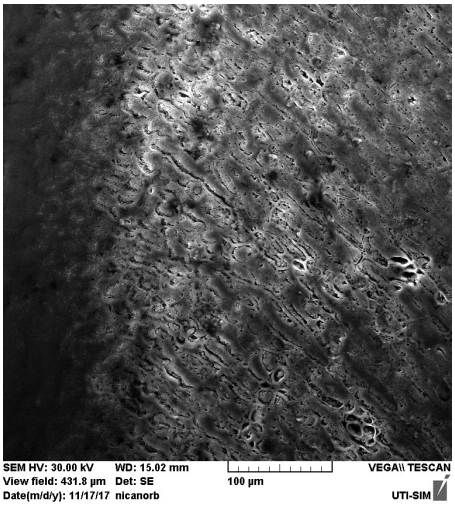

(**f**)

Figure 9. Microstructure in the cross-section of the MIG weld, magnification: (**a**) 100×, without vibrations; (**b**) 100×, with vibrations; (**c**) 200×, without vibrations; (**d**) 200×, with vibrations; (**e**) 500×, without vibrations; (**f**) 500×, with vibrations.

It can be seen that within the bands, the concentrations of silicon and copper are increased, especially in the MIG welds obtained with the participation of vibrations. At the nodes of the vibration wave, the structure appeared to be more advantageous than at its maximum. It can be seen in Figure 4 that Si and Cu have precipitated from the solid solution. This effect occurs in both displacements.

3.3. Hardness Determination of Specimens

The hardness of the aluminum alloys can be influenced by variables which include microstructural elements, chemical composition and strength. Vickers HV microhardness (100 g) was established using microhardness equipment (FUTURE-TECH, Kawasaki, Japan) which allows micrometer measurements using a force of up to 1000 g. The software analyses the structure according to the change in hardness and exerts a force of 100 g for 10 s. For each sample, three measurements were performed in the heat-affected layer and in the base material. The results presented in the tables below represent the average of the measurements.

3.3.1. Welded Specimens Without Longitudinal Vibrations

Tables 7 and 8 present the microhardness determinations for the welded specimens without longitudinal vibrations:

Table 7. Microhardness in the HAZ of the welded specimens without longitudinal vibrations.

Place of Indentation	HV100 gf	Imprint Size Diag.x	Imprint Size Diag.y
HAZ	97.8	0.0467 µm	0.0404 µm

Table 8. Microhardness in the weld without longitudinal vibrations.

Place of Indentation	HV100 gf	Imprint Size Diag.x	Imprint Size Diag.y
Weld	75.8	0.0511 µm	0.0484 µm

3.3.2. Welded Specimens with Forced Longitudinal Vibrations

Tables 9 and 10 present the microhardness determinations for the welded specimens with forced longitudinal vibrations:

Table 9. Microhardness in the HAZ of the welded specimens with forced longitudinal vibrations.

Place of Indentation	HV100 gf	Imprint Size Diag.x	Imprint Size Diag.y
HAZ	110	0.0447 µm	0.0376 µm

Table 10. Microhardness in the weld with forced longitudinal vibrations.

Place of Indentation	HV100 gf	Imprint Size Diag.x	Imprint Size Diag.y
Weld	82.4	0.0527 µm	0.0422 µm

3.4. Transverse Tensile Test of Welds

The tensile laboratory tests were performed at ambient temperature (24 °C) and in accordance with EN ISO 4136: 2013 [83]. In Figure 10 the specimens are shown after the tensile test was performed. In Figure 10a the test pieces presented are welded on a static surface. In Figure 10b the test pieces presented are welded with longitudinal vibration. As the images show, in both welding procedures the specimens were torn as expected, inside the structure of the weld, near the HAZ. This result can have multiple causes, but in this particular condition, the authors have to take into consideration the metallographic changes that occur in the molten pool based on two alloys with a completely different behavior on welding, which are set to highlight the level of impact imposed by two opposite welding conditions.

(**a**)

(**b**)

Figure 10. Test pieces: (**a**) welded on a static surface; (**b**) welded with longitudinal vibration.

In accordance with EN 485-2: 2016 [84], the tensile strength of the AlZn5.5MgCu alloy is 540 MPa compared to 180 MPa for AlSi5, factors which determine that the yield point will be in the weld not in the base material. The results for the tensile tests on both procedures are presented in the figures below. Figure 11 depicts the graphs for the test specimens welded without vibrations.

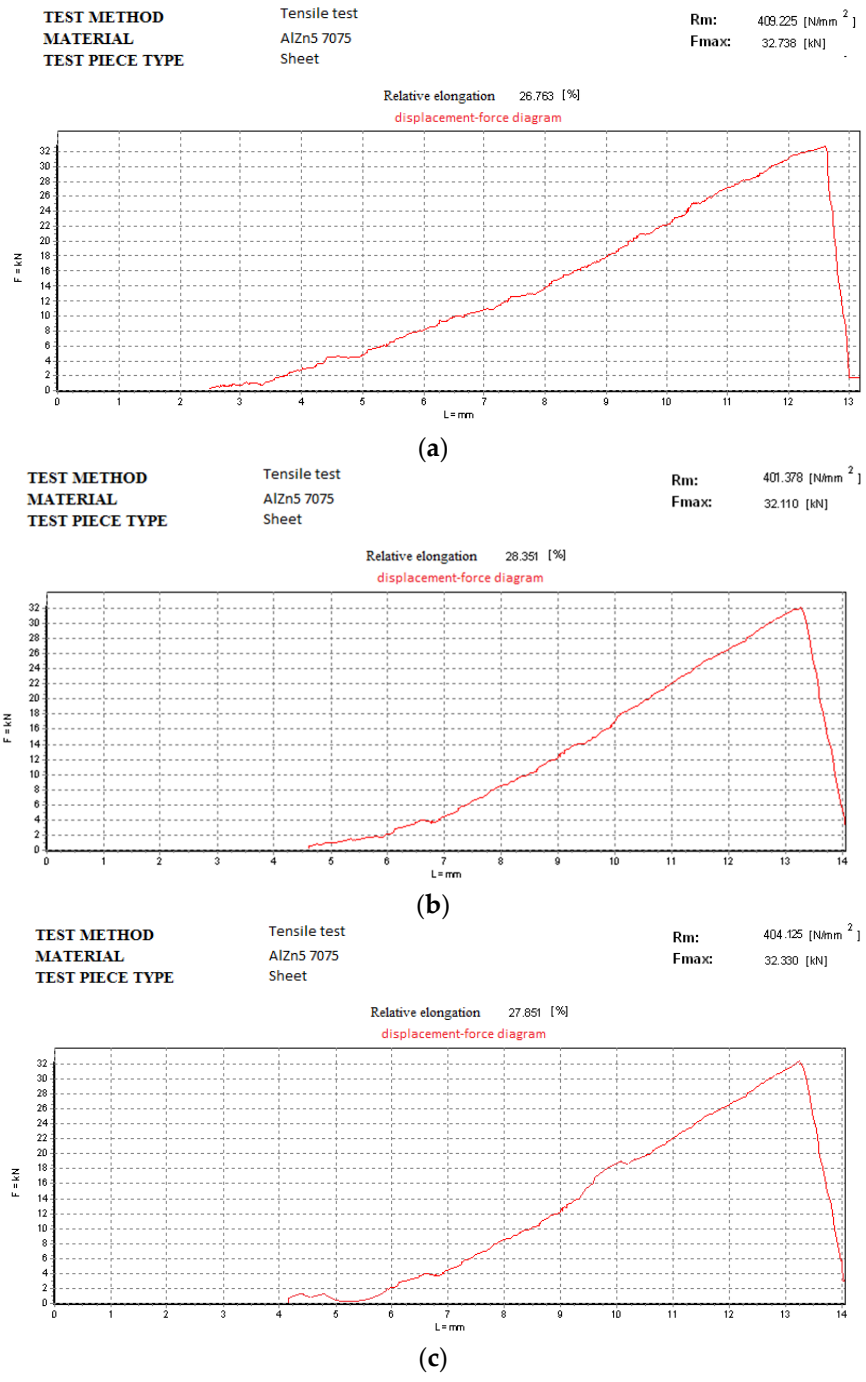

Figure 11. Tensile test for the specimens welded without vibrations: (**a**) test piece 1; (**b**) test piece 2; (**c**) test piece 3 from Figure 10a.

For the test pieces welded without vibrations (Figure 11) the authors obtained the following values: (a) 409.225 N/mm^2 for test piece 1; (b) 401.378 N/mm^2 for test piece 2; (c) 404.125 N/mm^2 for test piece 3. Figure 12 depicts the graphs for the test specimens welded on a vibrating surface. In both cases the test specimen broke at similar forces for their specific procedure.

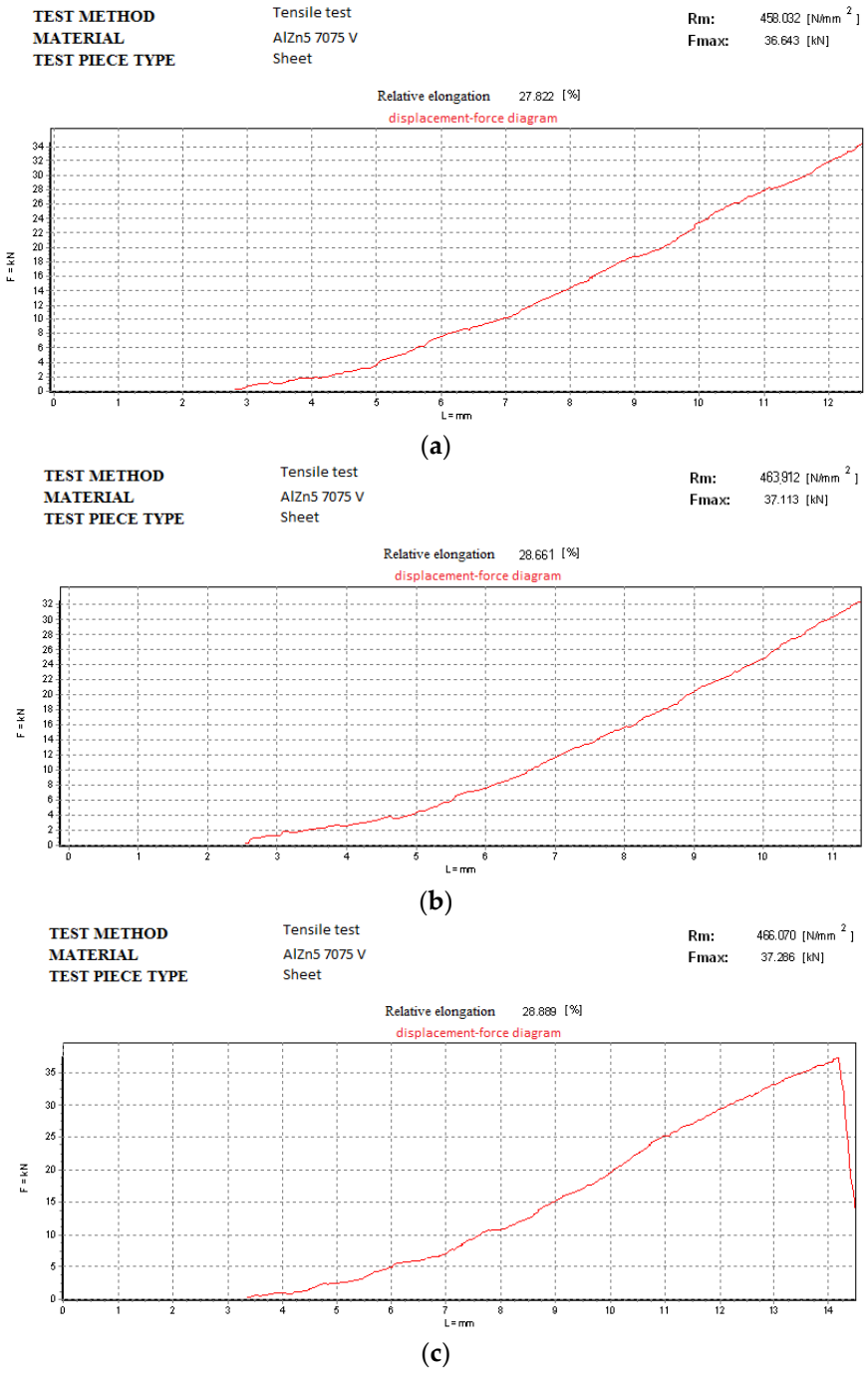

Figure 12. Tensile test for the specimens welded with vibrations: (**a**) test piece 1; (**b**) test piece 2; (**c**) test piece 3 from Figure 10b.

For the test pieces welded with vibrations (Figure 12) the authors obtained the following values: (a) 458.032 N/mm^2 for test piece 1; (b) 463.912 N/mm^2 for test piece 2; (c) 466.070 N/mm^2 for test piece 3.

3.5. Energy-Dispersive X-Ray Spectroscopy

Energy-Dispersive X-ray Spectroscopy (EDX, TESCAN, Brno, Czech Republic) analysis can provide the chemical characterization of each specimen, as seen in Figures 3 and 4. It can also highlight precipitation phenomena, which is the reason for applying this method.

4. Conclusions

This paper presents a comprehensive experimental study that aims to characterize and analyze the microstructural and mechanical properties of an Al 7075 alloy welded with MIG both without and with forced longitudinal vibrations, using the Al 4043 alloy as filler material. The use of forced longitudinal vibrations represents a heat treatment that is applied during welding, which does not require other post-welding treatments.

As a consequence of using Al 4043 as filler material, the HAZ becomes strengthened through precipitation during welding, especially due to additions of Mg and Cu. By introducing forced longitudinal vibrations in to the weld, the risk of hot cracking can be mitigated, and thus we obtain a lower level of hydrogen inclusions in a higher-density grain microstructure (fragile Mg_2Si grains). This results from the chemical composition concentrations, elemental mapping and EDX analysis provided in this study.

The microscopic observations, consisting in applying SEM on the HAZ and cross-section of the welds, have shown that the welds have a band structure, especially after the MIG processes are performed. Although welding of aluminum alloys encounters difficulties in regard to the removal of aluminum oxide, when mechanical vibrations are conducted as described in this study and highlighted by using SEM, an acceptable structure free of the characteristic porosity can be obtained.

The determinations for hardness performed in this study reveal an increase in Vickers HV on the cross-sections of the weld, performed under vibrations, by 8.7% and an increase of 12.5% in the HAZ of the same weld under vibrations compared to no vibrations being applied.

According to the data obtained for the tensile tests performed within this study, the authors notice an increase of 12–15.5% in tensile strength for the aluminum plates welded under longitudinal vibrations compared to no vibrations being applied.

Through grain structure growth and formation, it is possible to identify how alloy properties are influenced during welding. By controlling the nucleation and solidification process to a certain extent when welding, it is possible to modify the microstructural characteristics and consequently the mechanical properties of the weld. By technological optimization of the manner in which the metal pool is solidified (crystallizes), the authors show that alloys with low weldability can offer a specific set of properties that can prove to be appropriate. By inducing forced longitudinal vibrations, transmitted along the formation of the metal bed during welding, dissolved gasses are released and the grain density increases. The changes obtained are due to the influence of the frequency level, which alters the structure both in the fusion zone and in the middle of the weld, thus increasing the hardness. The aim of this research was to emphasize the differences between the effects of vibrations in MIG-welded Al 7075 (AlZn5.5MgCu) alloy specimens and the classic MIG welding procedure (without vibrations).

Author Contributions: Conceptualization, T.M.-P.; methodology, T.M.-P. and M.M.-P.; software, T.M.-P. and M.M.-P.; validation, T.M.-P. and M.M.-P.; formal analysis, M.M.-P.; investigation, T.M.-P. and M.M.-P.; resources, T.M.-P.; data curation, M.M.-P.; Writing—original draft preparation, T.M.-P.; writing—review & editing, M.M.-P.; visualization, T.M.-P. and M.M.-P.; supervision, T.M.-P.; project administration, T.M.-P.; funding acquisition, T.M.-P. All authors have read and agreed to the published version of the manuscript.

Funding: This research received no external funding.

Institutional Review Board Statement: Not applicable.

Informed Consent Statement: Not applicable.

Data Availability Statement: The original contributions presented in this study are included in the article. Further inquiries can be directed to the corresponding author.

Conflicts of Interest: The authors declare no conflict of interest.

References

1. Knap, A.; Dvořáčková, Š.; Váňa, M. Creation of an Aluminum Alloy Template with a Surface Structure by Micro-Milling for Subsequent Replication of the Microstructure to Achieve Hydrophobicity. *J. Manuf. Mater. Process.* **2024**, *8*, 26. [CrossRef]
2. Zhang, L.; Xing, S.; Zhai, H.; Hou, H.; Wang, Z.; Liu, S. Influence of Retrogression and Re-Aging Parameters on the Microstructure and Hardness of Jet-Formed 7050 Alloy. *Materials* **2025**, *18*, 1063. [CrossRef]
3. Tang, M.; Zhang, L.; Shi, Y.; Zhu, W.; Zhang, N. Research on the Improvement Effect and Mechanism of Micro-Scale Structures Treated by Laser Micro-Engraving on 7075 Al Alloy Tribological Properties. *Materials* **2019**, *12*, 630. [CrossRef] [PubMed]
4. Mirski, Z.; Ciepacz, I.; Wojdat, T. Soldering of 7075 Aluminum Alloy Using Ni-P and Cu-Cr Electrodeposited Interlayers. *Materials* **2020**, *13*, 4100. [CrossRef]
5. Li, Z.; Ou, L.; Wang, Y.; Li, H.; Bober, M.; Senkara, J.; Zhang, Y. Solidification Cracking Restraining Mechanism of Al-Cu-Mg-Zn Alloy Welds Using Cold Metal Transfer Technique. *Materials* **2023**, *16*, 721. [CrossRef] [PubMed]
6. Wang, X.; Zhang, D.; Li, A.; Yi, D.; Li, T. A Review on Traditional Processes and Laser Powder Bed Fusion of Aluminum Alloy Microstructures, Mechanical Properties, Costs, and Applications. *Materials* **2024**, *17*, 2553. [CrossRef]
7. Cabral-Miramontes, J.; Almeraya-Calderón, F.; Méndez-Ramírez, C.T.; Flores-De los Rios, J.P.; Maldonado-Bandala, E.; Baltazar-Zamora, M.Á.; Nieves-Mendoza, D.; Lara-Banda, M.; Pedraza-Basulto, G.; Gaona-Tiburcio, C. Effect of Citric Acid Hard Anodizing on the Mechanical Properties and Corrosion Resistance of Different Aluminum Alloys. *Materials* **2024**, *17*, 4285. [CrossRef]
8. Navaneethakrishnan, K.; Veeramani, A.; Chigilipalli, B.K.; Cheepu, M. Synthesis and Characterization of Recycled-TiC Reinforced AlZnMgCu Powder Metallurgy Composites. *Materials* **2024**, *17*, 4773. [CrossRef] [PubMed]
9. Choi, G.; Chae, H.; Kim, Y.S.; Hong, S.-K.; Shin, E.; Lee, S.Y. Additive Manufacturing of Si-Added 7075 Aluminum Alloys: Microstructural, Mechanical, and Electrochemical Properties via Heat Treatment. *Materials* **2025**, *18*, 1544. [CrossRef]
10. Lu, Z.; Wu, X.; Xu, J.; Zhang, H.; Yu, L.; Zhao, L.; Jiang, Y. Improving mechanical properties of spray formed 7055 aluminium alloy metal-inert gas welds by scandium addition. *J. Alloys Compd.* **2025**, *1013*, 178406. [CrossRef]
11. Zhang, B.; Zhang, Y.; Zheng, K.; Chi, Y. Research on the microstructure, mechanical and fatigue performance of 7075/6061 dissimilar aluminum alloy fusion welding joint treated by nanoparticle and post-weld heat treatment. *Eng. Fract. Mech.* **2024**, *311*, 110550. [CrossRef]
12. Dixit, S.; Liu, S. Laser Additive Manufacturing of High-Strength Aluminum Alloys: Challenges and Strategies. *J. Manuf. Mater. Process.* **2022**, *6*, 156. [CrossRef]
13. Satputaley, S.S.; Waware, Y.; Ksheersagar, K.; Jichkar, Y.; Khonde, K. Experimental investigation on effect of TIG welding process on chromoly 4130 and aluminum 7075-T6. *Mater. Today: Proc.* **2021**, *41*, 991–994. [CrossRef]
14. Zhong, S.; Han, S.; Chen, J.; Ren, J.; Zhou, Z.; Wen, F.; Qi, L.; Guan, R. Microstructure and properties of 7075 aluminum alloy welding joint using different filler metals. *Mater. Today Commun.* **2022**, *31*, 103260. [CrossRef]
15. Hassanifard, S.; Varvani-Farahani, A. A Comparative Study on Fatigue Response of Aluminum Alloy Friction Stir Welded Joints at Various Post-Processing and Treatments. *J. Manuf. Mater. Process.* **2021**, *5*, 93. [CrossRef]
16. Joshi, A.; Gope, A.; Chandra Gope, P. Effect of post-weld heat treatment on mechanical properties and fatigue crack growth behaviour of friction stir welded 7075-T651 Al alloy. *Theor. Appl. Fract. Mech.* **2023**, *123*, 103714. [CrossRef]
17. Chen, F.; Liu, C. Improving the Properties of Laser-Welded Al–Zn–Mg–Cu Alloy Joints by Aging and Double-Sided Ultrasonic Impact Compound Treatment. *Materials* **2021**, *14*, 2742. [CrossRef]
18. Niu, P.; Li, W.; Yang, C.; Chen, Y.; Chen, D. Low cycle fatigue properties of friction stir welded dissimilar 2024-to-7075 aluminum alloy joints. *Mater. Sci. Eng. A* **2022**, *832*, 142423. [CrossRef]
19. Wang, H.; Xu, W.; Wang, Y.; Lu, H. Creep-fatigue behavior of a friction stir welding 7050-T7451 aluminum alloy: Microstructure evolution and microscopic damage mechanisms. *Int. J. Fatigue* **2025**, *194*, 108840. [CrossRef]
20. Tahmasbi, A.; Moungomo, J.B.M.; Samuel, A.M.; Zedan, Y.; Songmene, V.; Samuel, F.H. Role of Li and Sc Additions and Machining Conditions on Cutting Forces on Milling Behavior of A7075-Based Alloys. *J. Manuf. Mater. Process.* **2024**, *8*, 83. [CrossRef]
21. Li, G.; Chen, F.; Han, Y.; Liang, Y. Improving Mechanical Properties of PVPPA Welded Joints of 7075 Aluminum Alloy by PWHT. *Materials* **2018**, *11*, 379. [CrossRef]
22. Heiland, S.; Milkereit, B.; Hoyer, K.-P.; Zhuravlev, E.; Kessler, O.; Schaper, M. Requirements for Processing High-Strength AlZnMgCu Alloys with PBF-LB/M to Achieve Crack-Free and Dense Parts. *Materials* **2021**, *14*, 7190. [CrossRef] [PubMed]

23. Shen, Z.; Wu, Z.; Wang, T.; Jia, T.; Liu, C. Effect of Heat Treatment Processes on the Microstructure and Mechanical Properties of High-Strength Aluminum Alloy Deposited Layers Processed by Fused Arc Additive Manufacturing. *Materials* **2023**, *16*, 6801. [CrossRef]
24. Wang, K.; Naumov, A.; Panchenko, E.; Panchenko, O. A Review on Friction Stir Welding of High-Strength Al-Zn-Mg Alloy: Insights on Second-Phase Particles. *Materials* **2024**, *17*, 5107. [CrossRef] [PubMed]
25. Wang, Z.; Fan, X.; Zhang, Z.; Song, G.; Liu, L. Microstructure and mechanical properties of 7075-T6 aluminum alloy plates by welding with weld reinforcement rolling. *Mater. Sci. Eng. A* **2024**, *889*, 145854. [CrossRef]
26. Kumar Dewangan, S.; Kumar Tripathi, M.; Nandan Banjare, P.; Kumar Manoj, M. Temperature Distribution of Friction Stir Welded Al 7075 alloy using Finite Element Simulation along with Experimental Validation. *Mater. Today Proc.* **2023**. [CrossRef]
27. Ye, Z.; Zhu, H.; Wang, S.; Wang, W.; Yang, J.; Huang, J. Fabricate high-strength 7075 aluminum alloy joint through double pulse MIG welding process. *J. Manuf. Process.* **2024**, *125*, 512–522. [CrossRef]
28. Abdeltawab, N.M.; Elshazly, M.; Shash, A.Y.; El-Sherbiny, M. Studying the effect of processing parameters on the microstructure, strength, hardness, and corrosion characteristics of friction stir dissimilar welded AA5083 and AA7075 aluminum alloys reinforced with Al-SiC matrix. *Heliyon* **2025**, *11*, e41362. [CrossRef] [PubMed]
29. Silva, F.J.G.; Martinho, R.P.; Magalhães, L.L.; Fernandes, F.; Sales-Contini, R.C.M.; Durão, L.M.; Casais, R.C.B.; Sousa, V.F.C. A Comparative Study of Different Milling Strategies on Productivity, Tool Wear, Surface Roughness, and Vibration. *J. Manuf. Mater. Process.* **2024**, *8*, 115. [CrossRef]
30. Schönecker, R.I.E.; Baumann, J.; Garcia Carballo, R.; Biermann, D. Fundamental Investigation of the Application Behavior and Stabilization Potential of Milling Tools with Structured Flank Faces on the Minor Cutting Edges. *J. Manuf. Mater. Process.* **2024**, *8*, 174. [CrossRef]
31. Wu, H.; Lu, Z.; Hill, S.; Turner, R. Microstructure Characterisation and Modelling of Pre-Forging Solution Treatment of 7075 Aluminium Alloy Using Novel Heating Methods. *J. Manuf. Mater. Process.* **2024**, *9*, 2. [CrossRef]
32. Zhao, J.-R.; Hung, F.-Y.; Pan, C.-Y. Application of New Al-Si Welding Filler with High Concentration of Copper and Magnesium: High-Temperature Strength and Anti-Corrosion Mechanism. *Materials* **2023**, *17*, 126. [CrossRef] [PubMed]
33. Łastowska, O.; Starosta, R.; Jabłońska, M.; Kubit, A. Exploring the Potential Application of an Innovative Post-Weld Finishing Method in Butt-Welded Joints of Stainless Steels and Aluminum Alloys. *Materials* **2024**, *17*, 1780. [CrossRef]
34. Wu, C.; Wang, J.; Wang, Q.; Xia, P.; Li, D. 7075 aluminum alloy Friction Stir Welding (FSW): Quality analysis and mechanical properties with WC-Co tool. *Mater. Today Commun.* **2024**, *38*, 108203. [CrossRef]
35. Seyyed Afghahi, S.S.; Jafarian, M.; Paidar, M.; Jafarian, M. Diffusion bonding of Al 7075 and Mg AZ31 alloys: Process parameters, microstructural analysis and mechanical properties. *Trans. Nonferrous Met. Soc. China* **2016**, *26*, 1843–1851. [CrossRef]
36. Kim, J.-H.; Choi, H.-N.; Lee, K.-J.; Shin, J.; Seo, N.; Jung, J.-G.; Lee, S.-J.; Lee, S.-J. Effect of welding speed on microstructural evolution and strengthening mechanism of friction-stir welded 7075 aluminum. *Mater. Sci. Eng. A* **2024**, *908*, 146695. [CrossRef]
37. Hayat, F. Electron beam welding of 7075 aluminum alloy: Microstructure and fracture properties. *Eng. Sci. Technol. Int. J.* **2022**, *34*, 101093. [CrossRef]
38. Luo, G.; Cheng, M.; Liu, C.; Li, S.; Wang, X.; Song, L. Improving mechanical properties of quasi-continuous-wave laser beam welded 7075 aluminum alloy through microstructural refinement and homogenization of the fusion zone. *Opt. Laser Technol.* **2022**, *153*, 108221. [CrossRef]
39. Zhu, R.; Ji, X.; Yuan, B.; Liang, Z.; Du, P.; Zhang, L.; Xie, Z. Microstructure and mechanical properties of 7075 aluminum alloy welds by gas tungsten arc welding with trailing ultrasonic rotating extrusion. *J. Mater. Res. Technol.* **2024**, *33*, 1446–1459. [CrossRef]
40. Xing, W.; Yu, Z.; Zhou, J.; Zhang, Z.; Liu, C.; Zhao, H. Study of the friction stir welding process and mechanical behavior of 7075/6061 heterogeneous aluminum alloys based on in-situ EBSD/DIC testing. *Mater. Today Commun.* **2025**, *44*, 112000. [CrossRef]
41. Mehri, A.; Abdollah-zadeh, A.; Entesari, S.; Saeid, T.; Wang, J.T. The effects of friction stir welding on microstructure and formability of 7075-T6 sheet. *Results Eng.* **2023**, *18*, 101041. [CrossRef]
42. Kumar, R.; Singh Bhadauria, S.; Sharma, V.; Kumar, M. Effect on microstructure and mechanical properties of single pass friction stir welded aluminium alloy AA-7075-T651 joint. *Mater. Today Proc.* **2023**, *80*, 40–47. [CrossRef]
43. Liu, Y.; Li, J.; Xie, Z.; Chen, S.; Yang, J.; Huang, J.; Zhao, Z. Friction plug−riveting spot welding of AA 7075-T6 aluminum alloy and low carbon steel using 1045 steel rivet. *Trans. Nonferrous Met. Soc. China* **2024**, *34*, 3893–3904. [CrossRef]
44. Panwariya, C.; Dwivedi, D.K. Mechanistic insights into abnormal grain growth suppression in friction stir welded 7075-T651 aluminum alloys through variation in tool rotational speed. *Mater. Today Commun.* **2024**, *40*, 110133. [CrossRef]
45. Chen, Z.; Zhang, Y.; Chi, Y.; Gou, J.; Lin, C.; Lin, Y. Research on morphology, porosity, mechanical properties of 7075 aluminum alloy repaired by arc welding and laser shock forging. *Heliyon* **2023**, *9*, e22791. [CrossRef]
46. Shou, H.; Song, Y.; Zhang, C.; Zhang, P.; Zhao, W.; Zhu, X.; Shi, P.; Xing, S. Grain Structure and Texture Evolution in the Bottom Zone of Dissimilar Friction-Stir-Welded AA2024-T351 and AA7075-T651 Joints. *Materials* **2024**, *17*, 3750. [CrossRef]

47. Yuk, S.; Shim, S.H.; Jeong, M.; Lee, D.; Lee, K.; Kim, S.H.; Lee, S.Y.; Han, J.H. Micro/nanostructure evolution and deformation mechanisms in friction-stir-welded 7075 Al alloy: A comparative analysis of weld zones. *J. Mater. Res. Technol.* **2025**, *36*, 5193–5210. [CrossRef]
48. Xing, S.; Sun, J.; Zhang, C.; Shou, H.; Jia, L.; Lv, N. Effect of joining material direction on material flow, microstructure and mechanical properties of dissimilar AA2024/7075 joints fabricated by friction stir welding. *J. Mater. Res. Technol.* **2025**, *35*, 3679–3692. [CrossRef]
49. Joshani, E.; Beidokhti, B.; Davodi, A.; Amelzadeh, M. Evaluation of dissimilar 7075 aluminum/AISI 304 stainless steel joints using friction stir welding. *J. Alloys Metall. Syst.* **2023**, *3*, 100017. [CrossRef]
50. Wang, Z.; Zhang, Z.; Lang, Q.; Song, G.; Liu, L. Microstructure evolution and deformation behavior of TIG welded 7075-T6 aluminum alloy followed by partial hot rolling. *J. Manuf. Process.* **2023**, *94*, 524–538. [CrossRef]
51. Li, Z.; Zhang, Y.; Li, H.; Wang, Y.; Wang, L.; Zhang, Y. Liquation Cracking Susceptibility and Mechanical Properties of 7075 Aluminum Alloy GTAW Joints. *Materials* **2022**, *15*, 3651. [CrossRef]
52. Li, H.; Yan, W.; Li, Z.; Mariusz, B.; Senkara, J.; Zhang, Y. Numerical and experimental study of the hot cracking phenomena in 6061/7075 dissimilar aluminum alloy resistance spot welding. *J. Manuf. Process.* **2022**, *77*, 794–808. [CrossRef]
53. Guo, Y.; Ma, Y.; Zhang, X.; Qian, X.; Li, J. Study on residual stress distribution of 2024-T3 and 7075-T6 aluminum dissimilar friction stir welded joints. *Eng. Fail. Anal.* **2020**, *118*, 104911. [CrossRef]
54. Liu, X.; Ma, C.; Lu, S.; Xu, R.; Ma, K.; Liu, X.; Zhang, L. Elastic-plastic deformation and organization analysis for Al 7075 friction stir welding joints based on MXene/SWCNT sensor. *Sens. Actuators A Phys.* **2023**, *352*, 114203. [CrossRef]
55. Peta, K.; Stemp, W.J.; Stocking, T.; Chen, R.; Love, G.; Gleason, M.A.; Houk, B.A.; Brown, C.A. Multiscale Geometric Characterization and Discrimination of Dermatoglyphs (Fingerprints) on Hardened Clay—A Novel Archaeological Application of the GelSight Max. *Materials* **2025**, *18*, 2939. [CrossRef] [PubMed]
56. Ren, X.; Jiang, X.; Yuan, T.; Zhao, X.; Chen, S. Microstructure and properties research of Al-Zn-Mg-Cu alloy with high strength and high elongation fabricated by wire arc additive manufacturing. *J. Mater. Process. Technol.* **2022**, *307*, 117665. [CrossRef]
57. Remsak, K.; Boczkal, S.; Limanówka, K.; Płonka, B.; Żyłka, K.; Węgrzyn, M.; Leśniak, D. Effects of Zn, Mg, and Cu Content on the Properties and Microstructure of Extrusion-Welded Al–Zn–Mg–Cu Alloys. *Materials* **2023**, *16*, 6429. [CrossRef]
58. Joy, D.; Aravindakshan, R.; Varrma, N.S. Effect of Zirconium additions on microstructure and mechanical properties of hot rolled Al-Mg alloys. *Mater. Today Proc.* **2021**, *47*, 5098–5103. [CrossRef]
59. Derbiszewski, B.; Obraniak, A.; Rylski, A.; Siczek, K.; Wozniak, M. Studies on the Quality of Joints and Phenomena Therein for Welded Automotive Components Made of Aluminum Alloy—A Review. *Coatings* **2024**, *14*, 601. [CrossRef]
60. Borchers, T.E.; Seid, A.; Shafer, P.; Zhang, W. Exacerbated stress corrosion cracking in arc welds of 7xxx aluminum alloys. *Weld. World* **2018**, *62*, 783–792. [CrossRef]
61. Krajewski, A.; Włosiński, W.; Chmielewski, T.; Kołodziejczak, P. Ultrasonic-vibration assisted arc-welding of aluminum alloys. *Bull. Pol. Acad. Sci. Tech. Sci.* **2012**, *60*, 841–852. [CrossRef]
62. Dong, H.; Yang, L.; Dong, C.; Kou, S. Improving arc joining of Al to steel and Al to stainless steel. *Mater. Sci. Eng. A* **2012**, *534*, 424–435. [CrossRef]
63. Gould, J.E. Joining Aluminum Sheet in the Automotive Industry—A 30 Year History. *Weld. J.* **2012**, *91*, 23s–34s.
64. Bodeanu, M.A.; Machedon-Pisu, T. Increasing the Quality of Welded Joints of Al-Si 6082 Alloys by Introducing Forced Vibrations. *Mater. Sci. Forum* **2017**, *907*, 231–237. [CrossRef]
65. Zhu, S. Research on Thermal Process of MIG Welding of Aluminum Alloy with Longitudinal Magnetic Field. *Open Mech. Eng. J.* **2011**, *5*, 32–38. [CrossRef]
66. Zheng, P.; Lu, Q.; Zhang, P.; Yan, H.; Zhao, J.; Shi, H. Effect of Vibration on Microstructure and Fatigue Properties of 6082 CMT-Welded Joints. *Trans. Indian Inst. Met.* **2021**, *74*, 3217–3225. [CrossRef]
67. He, L.; Wu, M.; Li, L.; Hao, H. Ultrasonic generation by exciting electric arc: A tool for grain refinement in welding process. *Appl. Phys. Lett.* **2006**, *89*, 131504. [CrossRef]
68. Lei, Y.; Wang, Z.; Chen, X. Effect of arc-ultrasound on microstructures and mechanical properties of plasma arc welded joints of SiCp/Al MMCs. *Trans. Nonferrous Met. Soc. China* **2011**, *21*, 272–277. [CrossRef]
69. Dai, W.-L. Effects of high-intensity ultrasonic-wave emission on the weldability of aluminum alloy 7075-T6. *Materials Letters* **2003**, *57*, 2447–2454. [CrossRef]
70. Machedon-Pisu, T.; Magyari, M. Research on Cladding (CMT MIG, WIG Arc Mechanized Pulse) for Molds used for Casting. *Metal. Int.* **2013**, *18*, 89–94.
71. *SR EN 573-3:2014*; European Standard: Aluminium and Aluminium Alloys—Chemical Composition and Form of Wrought Products. Asociația de Standardizare din România (ASRO): Bucharest, Romania, 2014.
72. Park, H.J.; Rhee, S.; Kang, M.J.; Kim, D.C. Joining of Steel to Aluminum Alloy by AC Pulse MIG Welding. *Mater. Trans.* **2009**, *50*, 2314–2317. [CrossRef]

73. Raveendra, A.; Ravi Kumar, B.V.R.; Sivakumar, A.; Santhosh, N. Effect of Welding Parameters on 5052 Aluminium Alloy Weldments using TIG Welding. *Int. J. Innov. Res. Sci. Eng. Technol.* **2014**, *3*, 10302–10309. Available online: https://www.ijirset.com/upload/2014/march/56_Effect.pdf (accessed on 5 August 2025).
74. Arun, M.; Ramachandran, K. Effect of Welding Process on Mechanical and Metallurgical Properties of AA6061 Aluminium Alloy Lap Joint. *Int. J. Mech. Eng. Res.* **2015**, *5*, 163–178. Available online: https://www.ripublication.com/ijmer_spl/ijmaerv5n1spl_27.pdf (accessed on 6 August 2025).
75. da Silva, E.P.; Castro, C.A.C.; Correa, E.O. Joining of Ti6Al4V/Al7075-T6 alloys without forming an intermediate layer by the GMAW process. *Int. J. Adv. Manuf. Technol.* **2025**, *136*, 5083–5102. [CrossRef]
76. 4643 Aluminum Welding Wire: Alloy Description and Application. Available online: https://www.washingtonalloy.com/wp-content/uploads/2020/12/4643.pdf (accessed on 7 August 2025).
77. Qu, Z.; Han, T.; Cui, H.; Tang, X. A Comparison between Tungsten Inert Gas Welded Joints Welded by Commercial ER5183 Filler and Al–Mg–Zn–Sc–Zr–Mn Filler on Microstructure and Properties in 7075-T651 Aluminum Alloys. *Mater. Trans.* **2021**, *62*, 386–395. [CrossRef]
78. Norman, A.F.; Birley, S.S.; Prangnell, P.B. Development of new high strength Al—Sc filler wires for fusion welding 7000 series aluminium aerospace alloys. *Sci. Technol. Weld. Join.* **2003**, *8*, 235–245. [CrossRef]
79. Aluminum 5554. Available online: https://www.brazing.com/products/Welding_alloys/alloy5554.aspx (accessed on 8 August 2025).
80. Atabaki, M.M.; Nikodinovski, M.; Chenier, P.; Ma, J.; Harooni, M.; Kovacevic, R. Welding of Aluminum Alloys to Steels: An Overview. *J. Manuf. Sci. Prod.* **2014**, *14*, 59–78. [CrossRef]
81. 4043 vs. 5356: Key Differences in Aluminum Welding Filler Alloys. Available online: https://www.arccaptain.com/blogs/news/4043-vs-5356 (accessed on 9 August 2025).
82. Aluminum Filler Alloy: Selection Chart. Available online: https://esab.com/index.cfm/_api/render/file/?method=inline&fileID=7FEFED6B-E635-42AB-9B2D928603B0E235 (accessed on 12 August 2025).
83. *SR EN ISO 4136: 2013*; European Standard: Destructive Tests on Welds in Metallic Materials—Transverse Tensile Test. Asociația de Standardizare din România (ASRO): Bucharest, Romania, 2013.
84. *SR EN 485-2: 2016*; European Standard: Aluminium and Aluminium Alloys—Sheet, Strip and Plate Part 2: Mechanical Properties. Asociația de Standardizare din România (ASRO): Bucharest, Romania, 2016.